Dust Destruction in Type Ia SNRs in the Large Magellanic Cloud

B.J. Williams, K.J. Borkowski, S.P. Reynolds (NCSU), W.P. Blair, P. Ghavamian, R. Sankrit (JHU), R.C. Smith, S. Points (NOAO), K.S. Long (STScI), S. Hendrick (Millersville), J. Raymond (CfA), P.F. Winkler (Middlebury)

We present early results from an extensive survey of Magellanic Clouds supernova remnants (SNRs) with the Spitzer Space Telescope. We have obtained IR images of several type Ia SNRs in the Large Magellanic Cloud (LMC), with strong 24 micron detections of DEM L71, 0509-67.5, N103B, 0519-69.0, DEM L238, and 0548-70.4. A comparison of these images to Chandra broadband images shows a clear association with the blast wave, and not with internal X-ray emission associated with ejecta. Since emission for SNRs at these infrared wavelengths is primarily thermal radiation from dust heated by the plasma, we infer that little dust has formed in the SN ejecta; we are seeing ambient interstellar dust that has been swept up and heated by the main blast wave. We employ computer models for dust emission which use plasma parameters determined from X-ray analysis to predict fluxes at Spitzer wavelengths. We find that our models can only reproduce observed flux ratios from Spitzer's 24 and 70 micron cameras if dust grain destruction (sputtering) is included. Since grains are heated and sputtered by ions and electrons in the plasma, the plasma temperature and density must be determined from X-ray analysis, which, combined with the age of the remnant, give an estimate for the amount of dust sputtered. We find that the amount of dust present is much less than expected based on estimates for average dust abundance in the LMC.

SNR 0548-70.4

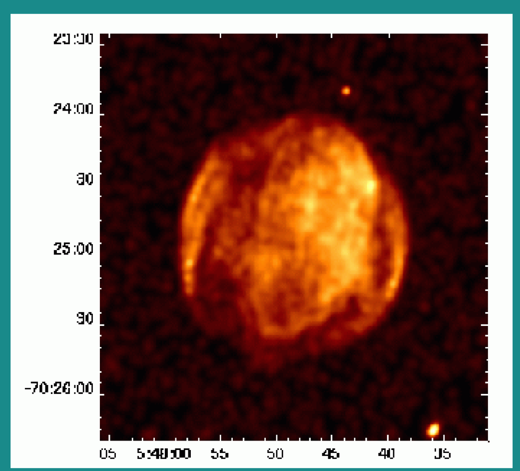

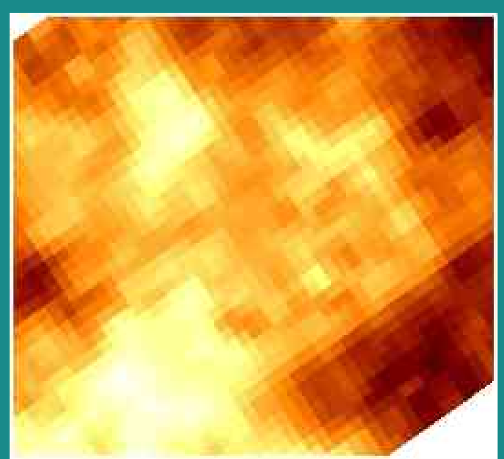

Top Left: Chandra (0.3-10 keV); **Top Right:** Spitzer 24-micron **Bottom Left:** Spitzer 70-micron Note the lack of clear interior emission in the infrared images, whereas the “wings” of the SNR can be identified in both wavelengths.

N103B (0509-68.7)

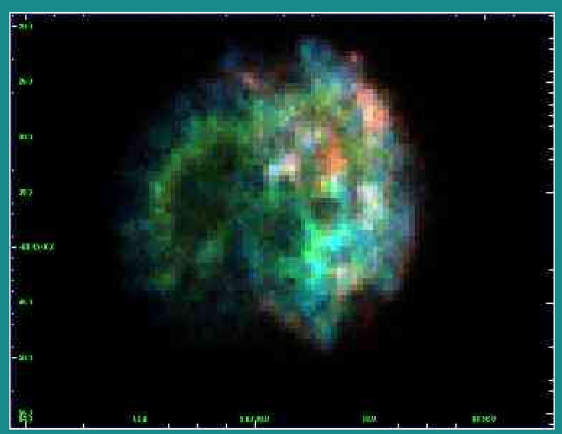
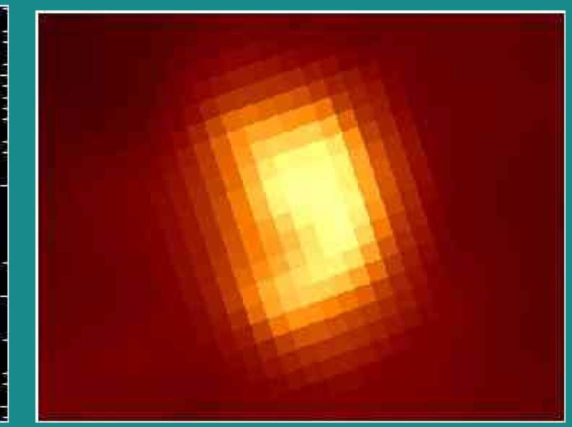
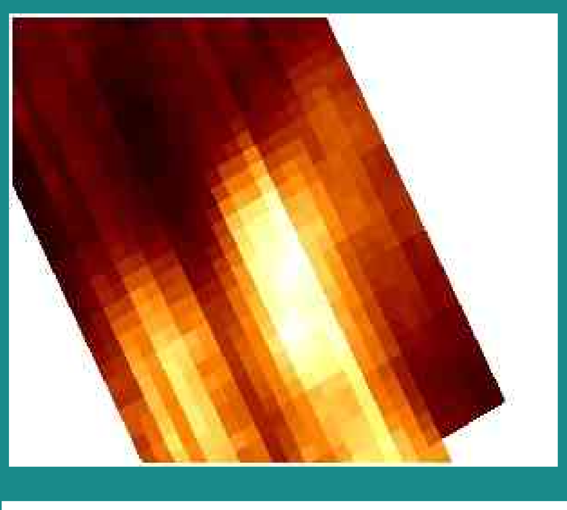


Top Left: Chandra (0.5-7.0 keV); **Top Right:** Spitzer 24-micron **Bottom Left:** Spitzer 70-micron; **Bottom Right:** Combined X-ray and IR, X-ray in blue, 24-micron IR in red.
N103B is well detected in both 24 and 70 microns by Spitzer, and there is a clear correlation between the west-side of the x-ray image and the detection in infrared. We fit a Sedov model to the western half of the remnant in x-rays, and extracted plasma parameters to use as inputs for dust models. An age of 860 years was used (Rest, et al. 2005). Results are summarized below.

T_e (keV)	T_p	n_0 (cm^{-3})	n_e	n_p	70/24 ratio (pred.)	70/24 (obs.)	Current Dust Mass (M_{Sun})	Orig. Mass
2	2	5	24	20	0.6	0.5	0.0015	0.0024

SNR 0509-67.5

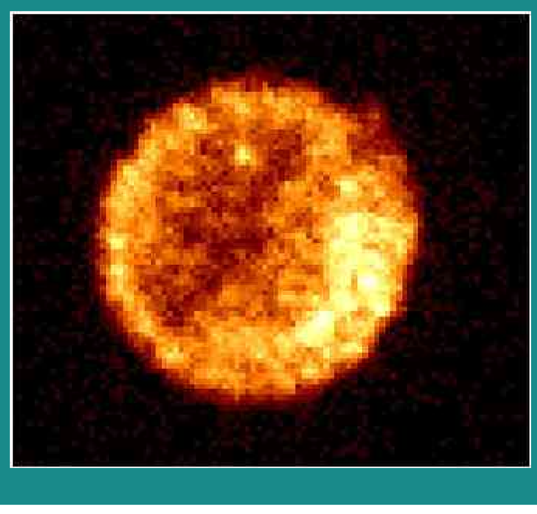
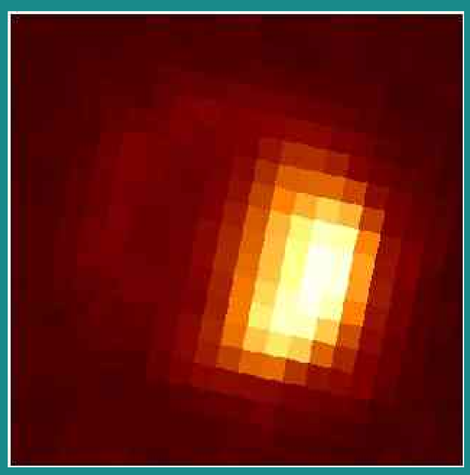

Left: Chandra (0.3-10 keV); **Right:** Spitzer 24 micron.
SNR 0509-67.5 is clearly detected in Spitzer, and shows association with X-ray morphology. Estimates for several different values of density were considered. Age was taken as 410 years (Rest, et al, 2005). This is approximately the same as Tycho's SNR. Results are summarized below.

Age (yr)	T_e (keV)	T_p	n_0 (cm^{-3})	n_e	n_p	70/24 ratio (pred.)	Current Dust Mass (M_{Sun})	Orig. Mass
410	0.96	50.4	0.1	0.48	0.4	6.38	0.01	0.011
410	1.36	41.9	0.3	1.44	1.2	2.9	0.0018	0.002
410	2.04	36.0	1.0	4.8	4.0	1.07	0.00027	0.00035

DEM L71 (0505-67.9)


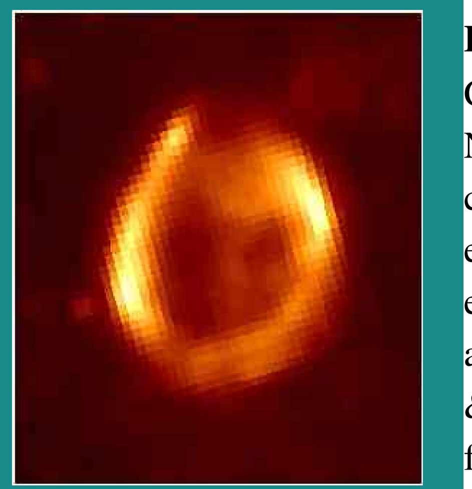

Top Left: Chandra (0.3-10 keV); **Top Right:** Spitzer 24-micron; **Bottom Left:** Spitzer 70-micron; **Bottom Right:** Combined X-ray and IR view of DEM L71. Chandra image is in blue, Spitzer 24-micron is in red. Note the clear correlation at the blast wave, whereas the center of the remnant is dominated by X-ray emitting ejecta. Ion and electron temperature and density were extracted from the Chandra data for several regions around the blast wave (Rakowski, Ghavamian, &Hughes, 2003). These parameters were used as input for dust emission models to predict fluxes in Spitzer wavelengths. The dust models also give a prediction for the total amount of dust in the remnant, which we compare with general predictions for the ISM in the Large Magellanic Cloud. Results are summarized in the table below. Our estimates for the swept up mass of DEM L71 is 110-130 solar masses, and with an average dust/gas mass ratio in the LMC of 0.003 (Weingartner & Draine, 2000), this gives a prediction for the mass of dust in DEM L71 of 0.36 solar masses. We find a total dust mass of 0.04 solar masses.
N.B. The remnant is divided up into 7 regions, moving clockwise around the shell from the upper right.

Region	T_e (keV)	T_p	n_0 (cm^{-3})	n_e	n_p	70/24 ratio (pred.)	70/24 (obs.)	Dust Mass (M_{Sun})
1	0.71	1.29	0.45	2.16	1.8	6.82	5.45	0.0035
2	0.64	1.0	0.54	2.6	2.17	5.36	3.1	0.0035
3	0.81	1.81	0.33	1.58	1.32	8.33	3.69	0.0055
4	0.66	1.18	0.48	2.3	1.92	6.77	6.7	0.0055
5	0.73	0.98	0.47	2.26	1.88	6.18	5.0	0.0024
6	0.63	1.0	0.4	1.9	1.6	6.82	3.5	0.011
7	0.42	0.36	1.3	6.24	5.2	3.44	3.2	0.0024

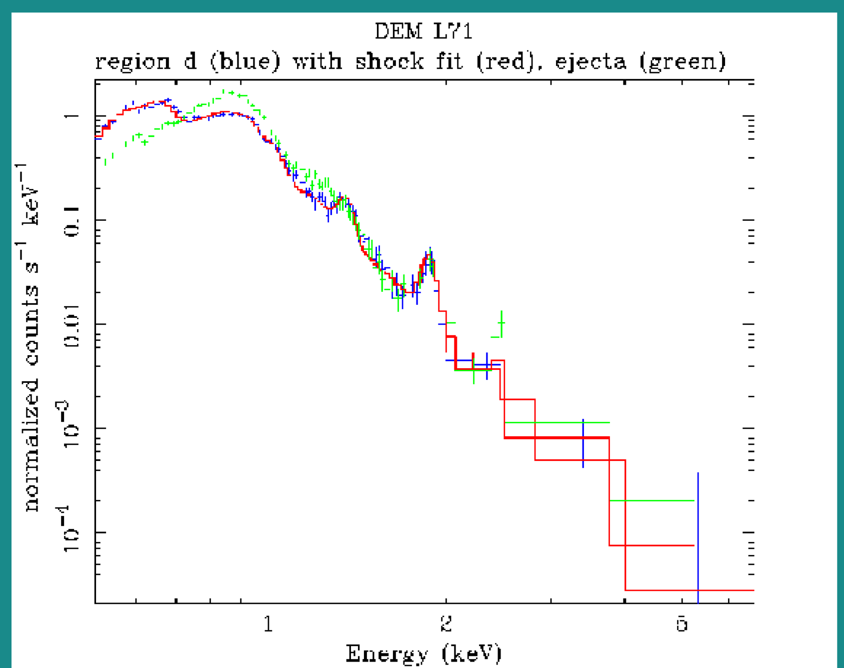

X ray spectra provide us with the post shock electron temperature and ionization age of the shock. We show here a plane shock fit to an X-ray spectrum of region 4, with the derived temperature of 0.700 keV, (0.888-0.713 keV 90% confidence) and the shock ionization age of $3.6(3.1-4.1) \times 10^{11}$ s cm^{-1}. Plasma conditions necessary for dust modeling can be determined accurately from X-ray spectra in this case. X ray spectra of Fe rich ejecta in Type Ia SNe are dominated by the Fe L-shell complex, and can be easily distinguished from the blast wave spectrum.

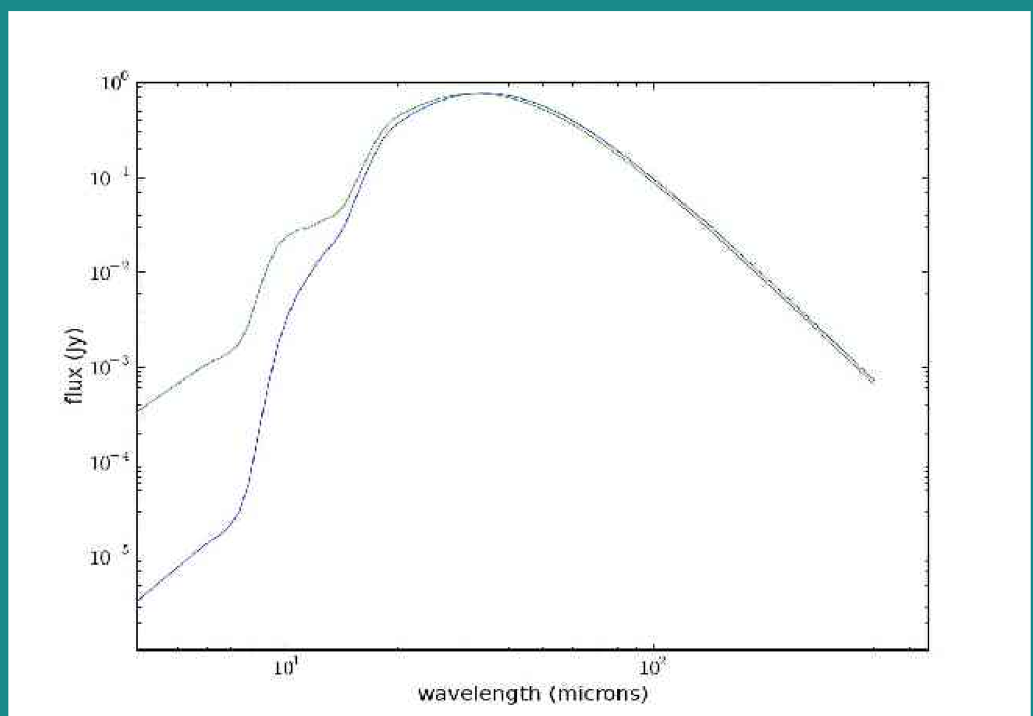

We have computer models that predict emission from collisionally-heated dust grains given the parameters of the energetic particles that are excited by the supernova blast wave. The output of our models is a spectrum. Dust grains emit a modified blackbody spectrum, with smaller grains radiating more in shorter wavelengths. We use a distribution of dust grain sizes in the LMC (Weingartner & Draine, 2000) and take different abundances of different types of grains (silicates, carbonaceous grains) into account. We calculate the amount of sputtering that occurs based on the temperature and density of energetic protons (Bianchi & Ferrera, 2005). We include the enhancement of sputtering of small grains in our models (Jurac, et al., 1998). Above is an example of an output from a model of dust in N103B. The green line is the spectrum that would be produced if there were no sputtering of dust grains, the blue line is what is produced when sputtering is taken into account. The difference is most significant at short wavelenghts, possibly explaining our lack of detection in the near-IR. The models take into account transient heating of small grains, which produces a different spectra than assuming constant temperature for grains.

DEM L238 (0534-70.5)

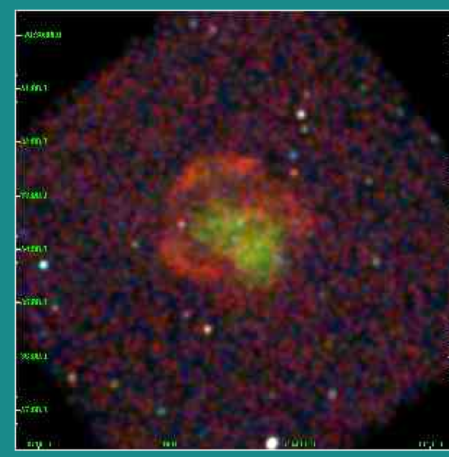
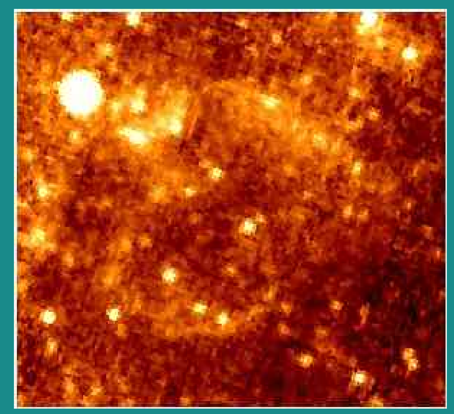

Left: Chandra (0.3-5 keV); **Right:** Spitzer 24-micron; The X-rays are dominated by ejecta in DEM L238, there is very little emission from the shock front. By contrast, the IR emission seems to be coming almost entirely from the blast wave, which is consistent with what we see in other remnants. Images not on the same scale.

SNR 0519-69.0


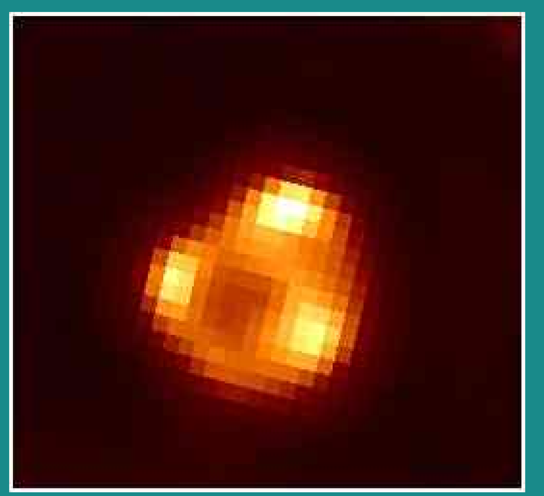
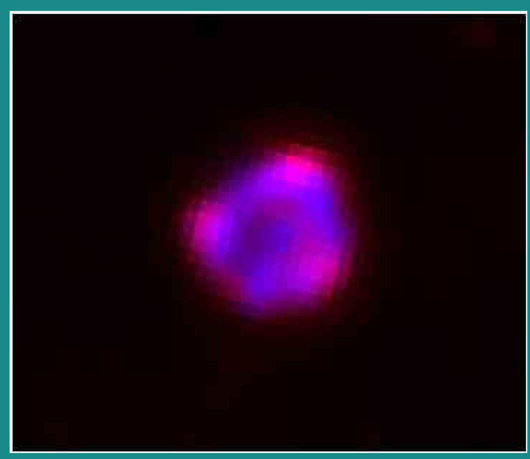

Top Left: Chandra (0.3-10 keV); **Top Right:** Spitzer 24-micron; **Bottom Left:** Combined X-ray and IR view of 0519-69.0. X-rays are in blue, 24-micron IR is in red.
SNR 0519-69.0 has an unusual morphology in X-rays and IR. Most interesting are the 3 bright knots in the 24-micron image. The estimated age of 0519 is 610 years (Rest, et al., 2005)

Conclusions

1. 24-micron IR emission shows an association with the blast wave, and not with the ejecta from the supernova. X-ray emission from ejecta can be distinguished from X-ray emission from the shock wave by analysis of Chandra spectra.

2. The amount of dust we calculate from IR observations is much less than expected based on estimates for the average dust/gas ratio in the LMC and estimates for the amount of swept up gas in these SNRs.

3. In those remnants with both 24 and 70 micron detections, our dust models can describe observed ratios reasonably well, but require the inclusion of sputtering (destruction) of small dust grains and transient heating.

4. A combined analysis of SNRs in infrared and X-rays provides a powerful diagnostic on plasma conditions that neither could provide on its own.

References

Bianchi, S. & Ferrera, A., 2005, MNRAS, 358, 379
Jurac, S., et al., 1998, ApJ, 503, 247
Rakowski, C., Ghavamian, P. & Hughes, J., 2003, ApJ, 590, 846
Rest, A., et al., 2005, Nature, in press
Weingartner, J. & Draine, B., 2001, ApJ, 548, 296